



Tumor cell-specific prodrugs using arsonic acid-presenting iron oxide nanoparticles with high sensitivity

Hiroki Minehara^a, Asako Narita^a, Kensuke Naka^b, Kazuo Tanaka^a, Moeko Chujo^c, Masaya Nagao^c, Yoshiki Chujo^{a,*}

^a Department of Polymer Chemistry, Graduate School of Engineering, Kyoto University, Katsura, Nishikyō-ku, Kyoto 615-8510, Japan

^b Department of Chemistry and Materials Technology, Graduate School of Science and Technology, Kyoto Institute of Technology, Sakyo-ku, Kyoto 606-8585, Japan

^c Division of Integrated Life Science, Graduate School of Biostudies, Kyoto University, Sakyo-ku, Kyoto 606-8502, Japan

ARTICLE INFO

Article history:

Received 3 April 2012

Revised 6 June 2012

Accepted 6 June 2012

Available online 15 June 2012

Keywords:

Arsonic acid

Iron oxide

Nanoparticle

Prodrug

Anticancer drug

ABSTRACT

We report the tumor cell-selective prodrugs based on the arsonic acid-presenting iron oxide nanoparticles. We synthesized the well-dispersed nanoparticles having arsonoacetic acid which is composed of the low toxic As(V) form. From the analyses of the reaction products, it is suggested that the reduction by dithiothreitol with arsonoacetic acid and the modified nanoparticles could generate the highly-toxic As(III) species. In the MTT assays, it was found that the cell viabilities of HeLaS3 and especially HepG2 were reduced in the presence of the modified nanoparticles. In contrast, a slight effect on viability was observed with primary mouse hepatocytes. The viabilities showed good agreements with the amounts of intracellular reduced glutathione concentrations. Furthermore, the valid concentrations of the modified nanoparticles for tumor-specific cytotoxicity were similar level in MRI measurements. These results indicate that arsonic acid-presenting nanoparticles should be a good platform for developing highly-sensitive tumor-specific prodrugs.

© 2012 Elsevier Ltd. All rights reserved.

1. Introduction

The biodistributions of iron oxide nanoparticles with approximately 10 nm of diameter can be readily tuned by the surface modifications.¹ For example, human serum albumin-tethered nanoparticles are accumulated at the tumor regions via the enhanced permeability and retention effect in which nanometer-sized macromolecules are specifically delivered to the tumor region.² Thereby, because of the superior effect to accelerate the transverse relaxation of water tissue in NMR measurements, they are applied as a contrast agent for cancer imaging and diagnosis. In addition, surface-modified iron oxide nanoparticles were also applied as vesicles for drug delivery and site-selective drug release. Various kinds of molecules are directly tethered to the surface and sustained at the surface modifications.^{3,4} By the target reactions or the micro-environmental changes, the sustained bio-active or probe molecules can be released.⁵ In particular, since the location of the nanoparticles is monitored by MRI, the releasing of the loaded drugs is readily confirmed.⁵ Hence, the protocols of the surface modification for functionalizing iron oxide nanoparticles are strongly desired for developing new series of the tumor-specific drug delivery and releasing system.

The differences of the environmental factors between tumor and normal cells are used as a trigger for activating prodrugs which must undergo chemical conversion by metabolic processes before becoming an active pharmacological agent, highly-specific anticancer drugs are developed, leading to the suppression of the administration amounts and undesired adverse effects.⁶ Reductive environments in the tumor cells were focused on the characteristics on tumor regions.^{7–9} Intracellular reductive environments are mainly controlled by modulating the amount of thiol groups in the reduced glutathione (GSH).^{10–12} Therefore, the thiol-responsive functional groups or molecules can be a candidate for the designs of the reduction-responsive prodrugs. Indeed, reductive environment-responsive prodrugs were developed not only for the imaging of cancer regions but also for anticancer drugs.

Organic arsenic compounds containing the As(V)–C bond are regarded as a reduction-responsive prodrug. In the presence of the reducing agent such as GSH, the transformation from As(V) to As(III) occurs with the bond cleavage of As–C, resulting in the generation of highly-toxic arsenic species.^{13,14} Since the concentrations of GSH in tumor cells are higher than those in normal cells, the transformation from As(V) to As(III) could be accelerated. Consequently, the tumor-selective cell death would be induced.^{15,16} However, there is still room to improve the specificity for biodistribution. In particular, effective accumulation of arsonic compounds should be necessary to suppress unexpectedly transformation to As(III) species before the localization at the target sites. Therefore,

* Corresponding author. Tel.: +81 75 383 2604; fax: +81 75 383 2605.

E-mail address: chujo@chujo.synchem.kyoto-u.ac.jp (Y. Chujo).

it should be of great significance to demonstrate the conjugation systems using arsonic compounds with other biocompatible materials.

Herein, we report the highly-sensitive anticancer prodrugs based on the arsonic acid-presenting iron oxide nanoparticles. We prepared arsonoacetic acid-tethered nanoparticles and investigated the reactivity with the thiol compound. It was found that the bond cleavage was induced between the As–C bond, leading to the generation of highly-toxic As(III) species. From the MTT assays, it was found that the significant decreases of cell viability were induced in the tumor cell lines in the presence of the modified nanoparticles with similar concentrations for MRI measurements. In addition, the degree of the toxicity showed good agreements with the intracellular GSH concentrations. Our findings propose that the arsonic acid can be a key functional group for developing a new series of prodrugs as anticancer agents with high sensitivity.

2. Experimental section

2.1. General

^1H NMR spectra were obtained with a JEOL EX-400 spectrometer (400 MHz). Transmission electron microscopy (TEM) was performed using a JEOL JEM-100SX operated at 100 kV electron beam acceleration voltage. One drop of the sample solution was deposited onto a copper grid and the excess of the droplet was blotted off the grids with filter paper. Subsequently the sample was dried under ambient conditions. Powder X-ray diffraction (XRD) patterns were recorded on a SHIMADZU X-ray diffractometer-6000 with high-intensity Cu K α radiation at a scanning rate of 0.02°S^{-1} in 2θ ranging from 2° to 90° . FT-IR spectra were recorded on a Perkin Elmer 1600 infrared spectrophotometer using a KBr disk dispersed with the powder sample. X-ray fluorescence (XRF) spectra were recorded on a Rigaku Primini with PdK α radiation ($\lambda = 0.05859 \text{ nm}$). The powder samples were used for XRD, FT-IR, XRF, and SQUID measurements. Dynamic light scattering (DLS) was measured to determine the hydrodynamic radii (r_{H}) of the samples on an FPAR-1000, Otsuka electronics Co., Ltd.

2.2. Materials

Iron(II) chloride hexahydrate, dithiothreitol and sodium hydride were purchased from Wako Pure Chemical Industries, Ltd (Osaka, Japan). Iron(III) chloride tetrahydrate was purchased from Kanto Chemicals Co., Ltd (Tokyo, Japan). All reagents were used as supplied, unless stated otherwise. Arsonoacetic acid was synthesized according to the previous work.¹⁷

2.3. Synthesis of the iron oxide nanoparticles

Preparation of the nanoparticles was according to our previous report.¹⁸ Iron(III) chloride hexahydrate (1.081 g, 4 mmol) and iron(II) chloride tetrahydrate (0.3976 g, 2 mmol) were dissolved in water (120 mL). After the addition of oleic acid (0.2 mL) with mechanically stirring at 1000 rpm, 15 mL of aqueous ammonium hydroxide (28%) was added to the solution all at once. Undecanoic acid (0.2 mL) was continuously added to the solution in four additions every 5 min with stirring at 1000 rpm at 80°C . After stirring for 30 min, the resulting dark brown suspension was cooled to room temperature. Undecanoic acid-coated nanoparticles (10 mg) were dispersed in toluene (2 mL), and arsonoacetic acid (27 mg) as a suspension in methanol (1 mL) was added under sonication. The dispersion was continuously sonicated overnight. The arsonic acid-presenting iron oxide nanoparticles were collected and washed with water five times using a magnet.

2.4. The evaluation of the number of arsonoacetic acid on the surface of particles

The standard samples with various concentrations were prepared by mixing naked SPIOs and arsonoacetic acid. Then, from the signal intensity of Fe, As and S elements in the XRF spectra, the standard curve was made. The ratios between Fe, As and S contents of the samples were calculated by fitting the observed values on the standard curves. From these procedure, we obtained 4.56 wt % of an As element as an average from the three samples. Therefore, 1 g of the sample contains 0.0456 g of an As element ($=0.112 \text{ g}$ of arsonoacetic acid and 0.888 g of Fe_3O_4). According to the density of Fe_3O_4 (5.18 g/cm^3)¹⁹ and the average radii of SPIO (ca. 4 nm), the molecular weight of the single SPIO particle is determined as 0.84 MDa. Then, it can be estimated that 1 g of the sample involves $1.06 \mu\text{mol}$ ($0.888/0.84 \text{ MDa}$) of SPIO and $610 \mu\text{mol}$ ($0.112/183.98$) of arsonoacetic acid. Finally, the number of arsonoacetic acid per the single particle was approximately determined as 570 ± 40 .

2.5. The reaction of arsonoacetic acid with dithiothreitol (DTT)

To the solution containing arsonoacetic acid (0.2 mmol) in D_2O (1.0 mL), DTT (0.2 or 0.4 mmol) was added and stirred at 40°C for 2 h. From the ^1H NMR spectra, conversions of arsonoacetic acid were determined from integral ratios between the methylene protons in arsonoacetic acid and the methyl protons in acetic acid.

2.6. The reaction of the modified nanoparticles with DTT

The modified nanoparticles (4 mg) were dispersed in water (10 mL) containing 10 mM or 100 mM DTT and stirred at 40°C for 2 h. The nanoparticles were collected by the magnets and washed with 20 mL of water five times. Then, the samples were dried in vacuo, and XRF analyses were executed to estimate the arsine content.

2.7. Cell viability assay

Primary mouse hepatocytes, HepG2, and HeLaS3 cells were used to test the toxic effects of various samples as assessed in the 3-[4,5-dimethylthiazol-2-yl]-2,5-diphenyltetrazolium bromide (MTT) assay. Cells were grown in Dulbecco's modified Eagle's medium (DMEM) containing 10% fetal bovine serum, 100 units/mL penicillin, 100 $\mu\text{g/mL}$ streptomycin and incubated at 37°C in humidified 5% CO_2 . Primary mouse hepatocytes were prepared by the method of collagenase perfusion²⁰ from 8 week-old male ICR mice. Briefly, livers were perfused at 37°C for 5 min with SC-1 solution consisting of 8000 mg/L NaCl, 400 mg/L KCl, 88.17 mg/L $\text{NaH}_2\text{PO}_4 \cdot 2\text{H}_2\text{O}$, 120.45 mg/L Na_2HPO_4 , 2380 mg/L HEPES, 350 mg/L NaHCO_3 , 190 mg/L EGTA, 900 mg/L glucose, pH 7.25, followed by digestion at 37°C for 6 min with 0.05% collagenase dissolved in SC-2 solution consisting of 8000 mg/L NaCl, 400 mg/L KCl, 88.17 mg/L $\text{NaH}_2\text{PO}_4 \cdot 2\text{H}_2\text{O}$, 120.45 mg/L Na_2HPO_4 , 2380 mg/L HEPES, 350 mg/L NaHCO_3 , 560 mg/L $\text{CaCl}_2 \cdot \text{H}_2\text{O}$, pH 7.25. The digested liver was excised, cut into small pieces and dispersed by pipetting. The resulting suspension was filtered through a $70 \mu\text{m}$ mesh and hepatocytes were collected by centrifugation at $50 \times g$ for 1 min. The cells were washed with DMEM 4 times and cultured in DMEM containing 10% fetal bovine serum and 10 nM dexamethasone. One day before the nanoparticle addition, HepG2 cells or HeLa S3 cells were seeded at 1500 cells/ $100 \mu\text{L}$ /well in a 96 well plate, while primary hepatocytes were seeded at 15,000 cells/ $100 \mu\text{L}$ /well. Three days after the cells were incubated with the modified nanoparticles, $10 \mu\text{L}$ of 5 mg/mL MTT in phosphate buffered saline was added to each well, and the plates were kept in

a CO₂ incubator for an additional 4 h. After MTT solution was removed, the cells were lysed by adding 100 μ l of 10% SDS, 0.01 M NH₄Cl and were incubated at 37 °C overnight. The degree of MTT reduction (i.e., cell viability) in each sample was subsequently assessed by measuring absorption at 600 nm using a plate reader. The absorbance values measured from the three wells were averaged, and the percentage MTT reduction was calculated by dividing this average by the absorbance measured from a control sample lacking the modified particles.

3. Results and discussion

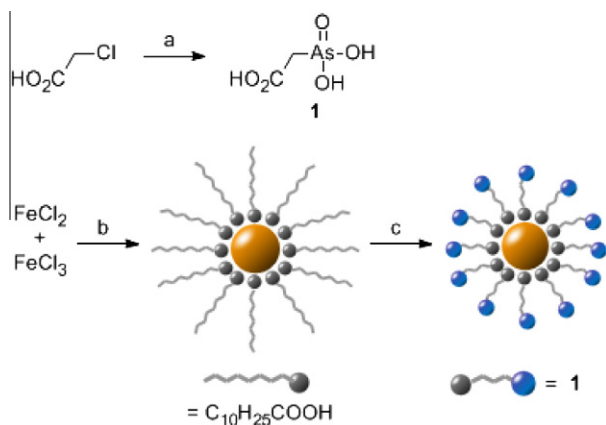
We designed the arsonoacetic acid-presenting iron oxide nanoparticles for highly-sensitive prodrugs. Iron oxide nanoparticles are a suitable platform to introduce the drugs into the cells by anchoring at the surfaces. In addition, the stable coordination of arsonoacetic acid to the surface of iron oxide can be formed using the carboxyl group and maintained under the biological conditions. Thereby, the arsonic acid moiety should be effectively accumulated into the cells. By transforming As(V) in $-\text{CH}_2\text{AsO}_3\text{H}_2$ group to As(III) by thiol groups, the highly-toxic arsenic species would be generated.^{13,14} Moreover, the minimum length of the aliphatic arsonic acid should hardly disturb the magnetic interaction between iron oxide and water tissue. Indeed, we have observed the clear contrast in T_2 -weighted MR images with higher sensitivity than that of the commercial contrast agent.^{21,22} Hence, arsonoacetic acid is the simple but highly-sophisticated molecules as a candidate for the prodrug which can be traced in MRI.

The arsonic acid-presenting nanoparticles were synthesized via the ligand exchange from undecanoic acid to arsonoacetic acid according to our previous report.¹⁸ The chemical structure of the modified nanoparticles is shown in Scheme 1. The identifications of the modified nanoparticles were executed with TEM and DLS for measuring the diameters ($7.6 \text{ nm} \pm 1.4 \text{ nm}$ from TEM, $9.4 \pm 2.4 \text{ nm}$ from DLS), and XRD. Elemental analysis and XRF spectroscopy suggested that the number of the arsonic acid presented from the single SPIO was approximately 600. It is reported that the interfacial areas of carboxylate were between 30 and 40 \AA^2 .^{23,24} From these facts, it is roughly estimated that the surface of the particles could be fully covered by arsonoacetic acid. It should be mentioned that by FT-IR measurements, arsonoacetic acid is confirmed to coordinate to the surfaces of the iron oxide particles at the carboxylic unit, but not at the arsonic acid unit. This means that arsonoacetic acid is immobilized onto the surface of the particles. The modified nanoparticles showed good dispersibility in

water. In addition, non-specific aggregation of the particles was hardly observed during the analyses.

Initially, the reaction products from arsonoacetic acid with the thiol compound were investigated. Ioannou et al. reported that thiols were able to break the C–As bond resulting in production of As(III) compounds.^{13,14} Correspondingly, the arsonic acid-containing liposomes were induced to show the strong toxicity triggered by the reduction leading to the arsenic acid releasing in the cells. Based on these facts, we evaluated the reaction products from the reductive degradation of arsonoacetic acid. Figure 1 represents the ¹H NMR spectra of the reaction solutions containing arsonoacetic acid in the presence of the same equivalent of DTT before and after 2 h incubation. The characteristic peak appeared at 1.9 ppm which could be assigned as the methyl group of acetic acid. In addition, the time-courses of the amounts of arsonoacetic acid were monitored in the presence of various concentrations of DTT (Table 1). The reaction yields were estimated with the ¹H NMR spectroscopy by calculating the conversion of arsonoacetic acid. The reactions completed by 2 h, and the observed conversion increased from 49% to 70% corresponded to the increase of the molar ratio of DTT against arsonoacetic acid. These results indicate that the reductive bond cleavage at the C–As bond, resulting in the production of highly-toxic arsenic compounds.

Same reactions were executed with the modified nanoparticles. The reactions were monitored with the XRF spectroscopy by evaluating the existence ratio of the C–As bond against the Fe–O bond. Figure 2 shows the XRF spectra of the modified nanoparticles before and after the treatment with DTT. The peak arising from AsK α was observed at $2\theta = 34^\circ$ before the reaction. On the other hand, the peak decreased after the reaction with 1 mM DTT. These data clearly indicate the bond cleavage between the C–As bond in arsonoacetic acid and the release of the arsenic element from the surface of the nanoparticles. In addition, from the measurements of the time-courses of the changes of arsenic element in the modified nanoparticles, the residual arsine content at the modified nanoparticles decreased to 33% by reacting with 1 mM DTT (Fig. 3). In the presence of 10 mM DTT, the residual arsine content further decreased to 22% after 2 h reactions. These data support the reductive bond cleavage between the C–As bond by DTT, leading to the generation of inorganic arsenic compounds. In particular, it is said that the intracellular concentrations of thiol groups are between 1 mM and 10 mM.^{10–12} Therefore, it can be presumed that the inorganic arsenic species were generated and showed the cytotoxicity in our experiments. To examine the coordination at the surfaces, the FT-IR spectra were measured (Fig. 4). The strong band at 579 cm^{-1} assigned as the Fe–O stretching vibrations related to the magnetic core was observed. The significant bands observed at 1100 cm^{-1} corresponding to As–O and As=O stretching vibrations disappeared after the reaction.²⁵ These results suggest the



Scheme 1. Synthesis and the chemical structure of the ligand used in this study. Reagents and conditions; (a) As₂O₃, water, 25 °C, 1 h; (b) oleic acid, undecanoic acid, NH₄OH, water, 80 °C, 30 min; (c) **1**, methanol, toluene, ultrasonic, rt, 16 h.

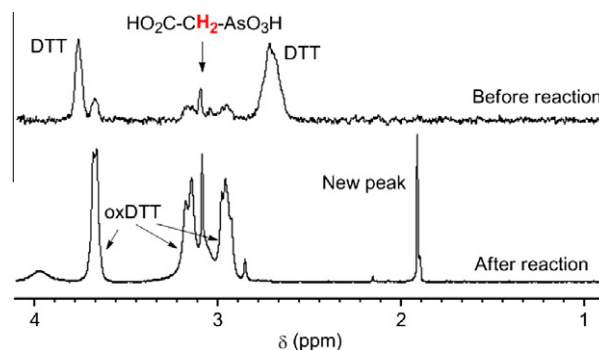


Figure 1. ¹H NMR spectra of the solutions (run 3) containing arsonoacetic acid and DTT in D₂O before and after 2 h incubation at 40 °C.

Table 1
Results of conversion of arsonoacetic acid to acetic acid in the presence of DTT

Run	DTT/1 (mol/mol)	Time (h)	Conversion (%)
1	1	1	27
2	1	2	47
3	1	5	49
4	2	1	49
5	2	2	68
6	2	5	70

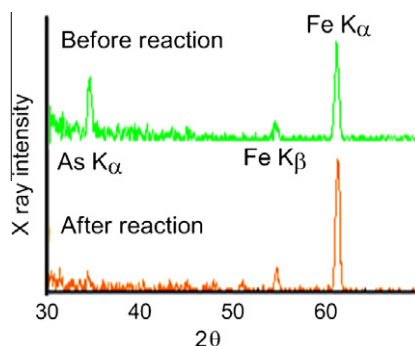


Figure 2. XRF spectra of the modified nanoparticles before and after reaction with 1 mM DTT.

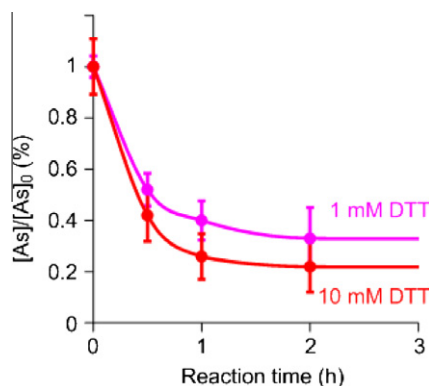


Figure 3. Time-courses of the changes of the residual arsine contents with the modified nanoparticles determined with XRF measurements after the reaction with DTT.

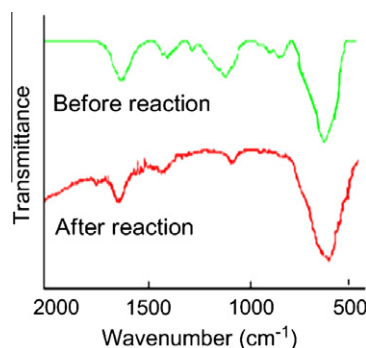
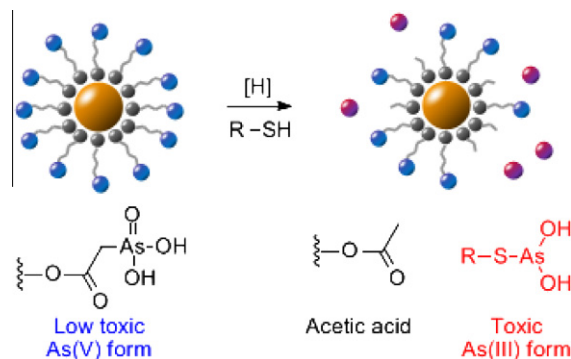


Figure 4. FT-IR spectra of the modified nanoparticles before and after reduction with DTT.

cleavage of the C–As bond and the generation of toxic inorganic arsenic acid species. The tumor-specific cytotoxicity could be triggered by reducing arsonoacetic acid. The relatively-higher reduc-



Scheme 2. Proposed reaction scheme of the reduction of arsonoacetic acid with DTT.

tive conditions in the tumor cells could enhance the generation of inorganic arsenic acid species. The bands corresponding to C=O stretching vibration were observed around 1400 cm^{-1} and 1600 cm^{-1} from both samples. This fact suggests that the coordination of carboxyl groups could be maintained during the reductive decomposition of arsonoacetic acid. These results are summarized as that the arsonoacetic acid at the surface of the iron oxide nanoparticles should be reduced by thiol groups and converted to acetic acid (Scheme 2).

The cytotoxicity of the modified nanoparticles was examined with three kinds of cells (HepG2, HeLaS3, and primary mouse hepatocytes). The MTT assays were executed in the presence of the modified nanoparticles, arsenic trioxide (As_2O_3) as a positive control, and the water-dispersive naked nanoparticles as a negative control with various concentrations. Figure 5 represents the cell viabilities after 72 h incubation with the samples. The strong toxicity was confirmed from As_2O_3 in all cells. The naked nanoparticles hardly affected the cell viability through the entire concentration range. Interestingly, the viabilities of the cancer cell lines (HepG2 and HeLaS3) significantly decreased in the presence of the modified nanoparticles. These data clearly indicate that arsonoacetic acid tethered to the nanoparticles should be responsible for cancer cell-selective cytotoxicity. Moreover, the viabilities were corresponded to the GSH concentrations of each cell line as previously reported (Table 2).^{7–9} It is strongly suggested that the reduction of As(V) to As(III) should occur and yield highly-toxic species. The cytotoxicity in HepG2 was obviously observed with $1\text{ }\mu\text{g/mL}$ of the modified nanoparticles. On the other hand, less significant effect on those of normal cells was observed even in the presence of 100-fold higher concentration than active one for HepG2. This concentration was a similar level to the detection limit of the conventional MRI contrast agents based on the iron oxide nanoparticles. These facts suggest that enough concentrations of the modified nanoparticles over the active amounts were obtained by the same administration manner with iron oxide nanoparticles used for an MRI contrast agent.

4. Conclusion

We demonstrate that the arsonic acid-presenting iron oxide nanoparticles have anti-cancer activity with high selectivity. The viabilities of the tumor cell lines as HepG2 and HeLaS3 were significantly reduced by adding the modified nanoparticles. On the other hand, the primary mouse hepatocytes were less affected even in the presence of 10-times. Such tumor cell-selective cytotoxicity could be explained by the intracellular concentrations of each cell line. The amount of GSH and the activities of GSH-relating enzymes are significant biomarkers such for apoptosis or responses of the vital cells toward stressful materials. Thus, the arsonic acid-based

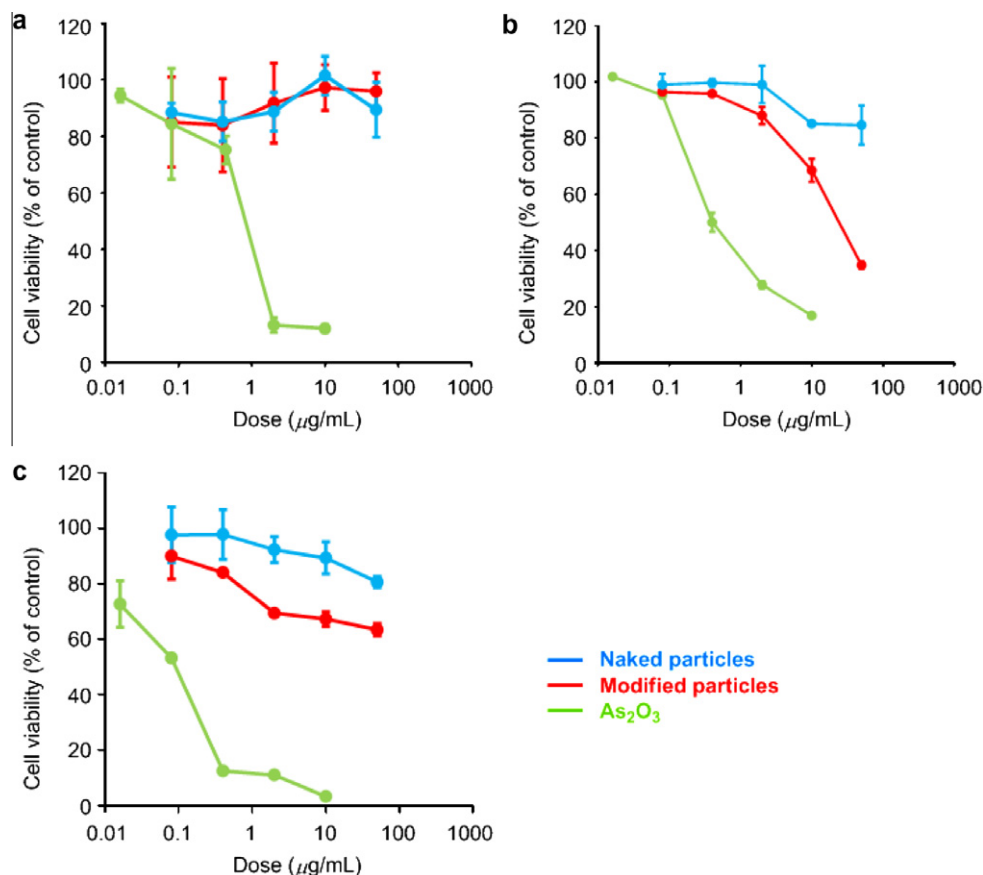


Figure 5. Effect of As_2O_3 , naked iron oxide nanoparticles, and the modified nanoparticles on the viability of normal cells ((a) primary mouse hepatocytes) and tumor cell lines ((b) HepG2 and (c) HeLaS3). Cells were incubated with various concentrations of the samples for 72 h. Results are expressed as viability (% viable cells in comparison with the control) versus the arsenic content for upper three graphs.

Table 2
GSH concentrations of three cell lines

Cell type	GSH concentration (nmol/mg)
HepG2	35.4 ^a
HeLa	13.4 ^b
Mouse primary hepatocyte	7 ^c

^a Ref. 7.

^b Ref. 8.

^c Ref. 9.

materials could be applied not only for monitoring these significant biological events but also for modulating cell activities using the reaction from As(V) to As(III) as a trigger.

References and notes

- Xie, J.; Liu, G.; Eden, H. S.; Al, H.; Chen, X. *Acc. Chem. Res.* **2011**, *44*, 883.
- Xie, J.; Chen, K.; Huang, J.; Lee, S.; Wang, J.; Gao, J.; Li, X.; Chen, X. *Biomaterials* **2010**, *31*, 3016.
- Hirata, N.; Tanabe, K.; Narita, A.; Tanaka, K.; Naka, K.; Chujo, Y.; Nishimoto, S. *Bioorg. Med. Chem.* **2009**, *17*, 3775.
- Naka, K.; Narita, A.; Tanaka, Y.; Chujo, Y.; Morita, M.; Inubushi, T.; Nishimura, I.; Hiruta, J.; Shibayama, H.; Koga, M.; Ishibashi, S.; Seki, J.; Kizaka-Kondoh, S.; Hiraoka, M. *Polym. Adv. Technol.* **2008**, *19*, 1241.
- Mornet, S.; Vasseur, S.; Grasset, F.; Dugnet, E. *J. Mater. Chem.* **2004**, *14*, 2161.
- Tanabe, K.; Harada, H.; Narazaki, M.; Tanaka, K.; Inafuku, K.; Komatsu, H.; Ito, T.; Yamada, H.; Chujo, Y.; Matsuda, T.; Hiraoka, M.; Nishimoto, S. *J. Am. Chem. Soc.* **2009**, *131*, 1598.
- Murakami, C.; Hirakawa, Y.; Inui, H.; Nakano, Y.; Yoshida, H. *Biosci. Biotechnol. Biochem.* **2002**, *66*, 1559.
- Toyoda, H.; Mizushima, T.; Satoh, M.; Iizuka, N.; Nomoto, A.; Chiba, H.; Mita, M.; Naganuma, A.; Himeno, S.; Imura, N. *Jpn. J. Cancer Res.* **2000**, *91*, 91.
- Ueno, S.; Susa, N.; Furukawa, Y.; Aikawa, K.; Itagaki, I.; Komiyama, T.; Takashima, Y. *Jpn. J. Vet. Sci.* **1988**, *50*, 45.
- Deneke, S. M.; Fanburg, B. L. *Am. J. Physiol.* **1989**, *257*, L163.
- Carmel-Harel, O.; Storz, G. *Annu. Rev. Microbiol.* **2000**, *54*, 439.
- Nordberg, J.; Arnér, E. S. J. *Free Radical Bio. Med.* **2001**, *31*, 1287.
- Ioannou, P. V.; Lala, M. A. *Appl. Org. Met. Chem.* **2000**, *14*, 261.
- Lala, M. A.; Ioannou, P. V. *J. Inorg. Biochem.* **2003**, *97*, 331.
- Gortzi, O.; Antimisariar, S. G.; Klepetsanis, P.; Papadimitriou, E.; Ioannou, P. V. *Eur. J. Pharm. Sci.* **2003**, *18*, 175.
- Gortzi, O.; Papadimitriou, E.; Kontoyannis, C. G.; Antimisariar, S. G.; Ioannou, P. V. *Pharm. Res.* **2002**, *19*, 79.
- Palmer, C. S. *J. Am. Chem. Soc.* **1923**, *45*, 3023.
- Minehara, H.; Naka, K.; Tanaka, K.; Narita, A.; Chujo, Y. *Bioorg. Med. Chem.* **2011**, *19*, 2282–2286.
- (a) Linde, D. R.; Frederikse, H. P. R. *Handbook of Chemistry and Physics*, 75th ed.; CRC: Boca Raton, FL, 1995; (b) Amstad, E.; Gillich, T.; Bilecka, I.; Textor, M.; Reimhult, E. *Nano Lett.* **2009**, *9*, 4042.
- Seglen, P. O. *Methods in Cell Biology*, In 2nd ed.; Preseon, D. M., Eds.; Academic Press: New York, 1976; Vol. 13, Chapter 4, pp 29–83.
- Tanaka, K.; Narita, A.; Kitamura, N.; Uchiyama, W.; Morita, M.; Inubushi, T.; Chujo, Y. *Langmuir* **2010**, *26*, 11759.
- Tanaka, K.; Kitamura, N.; Morita, M.; Inubushi, T.; Chujo, Y. *Bioorg. Med. Chem. Lett.* **2008**, *18*, 5463.
- Imae, T.; Takeshita, T.; Kato, M. *Langmuir* **2000**, *16*, 612.
- Naito, K.; Iwakiri, T.; Miura, A.; Azuma, M. *Langmuir* **1990**, *6*, 1309.
- Gründler, H.-V.; Schumann, H.-D.; Steger, E. *J. Mol. Struct.* **1974**, *21*, 149.